

RED-ACT Report

Real-time Earthquake Damage Assessment using City-scale Time-history analysis

May. 18, M5.0 Qiaojia, Yunnan Earthquake

Research group of Xinzheng Lu at Tsinghua University (luxz@tsinghua.edu.cn)

First reported at 22:30, May. 18, 2020 (Beijing Time, UTC +8)

Acknowledgments and Disclaimer

The authors are grateful for the data provided by **China Earthquake Network Center (CENC)**. This analysis is for research only. The actual damage resulting from the earthquake should be determined according to the site investigation.

Scientific background of this report can be found at: <http://www.luxinzheng.net/rr.htm>

1. Introduction to the earthquake event

At 21:47 May. 18 2020 (Local Time, UTC +8), an **M 5.0** earthquake occurred in **Qiaojia, Yunnan**. The epicenter was located at 27.18 103.16, with a depth of **8 km**.

2. Recorded ground motions

83 ground motions near to epicenter of this earthquake were analyzed. The names and locations of the stations can be found Table 1. The maximal recorded peak ground acceleration (PGA) is **315.64 cm/s/s**. The waveform and corresponding response spectra in comparison with the design spectra specified in the Chinese Code for Seismic Design of Buildings are shown in Figure 1.

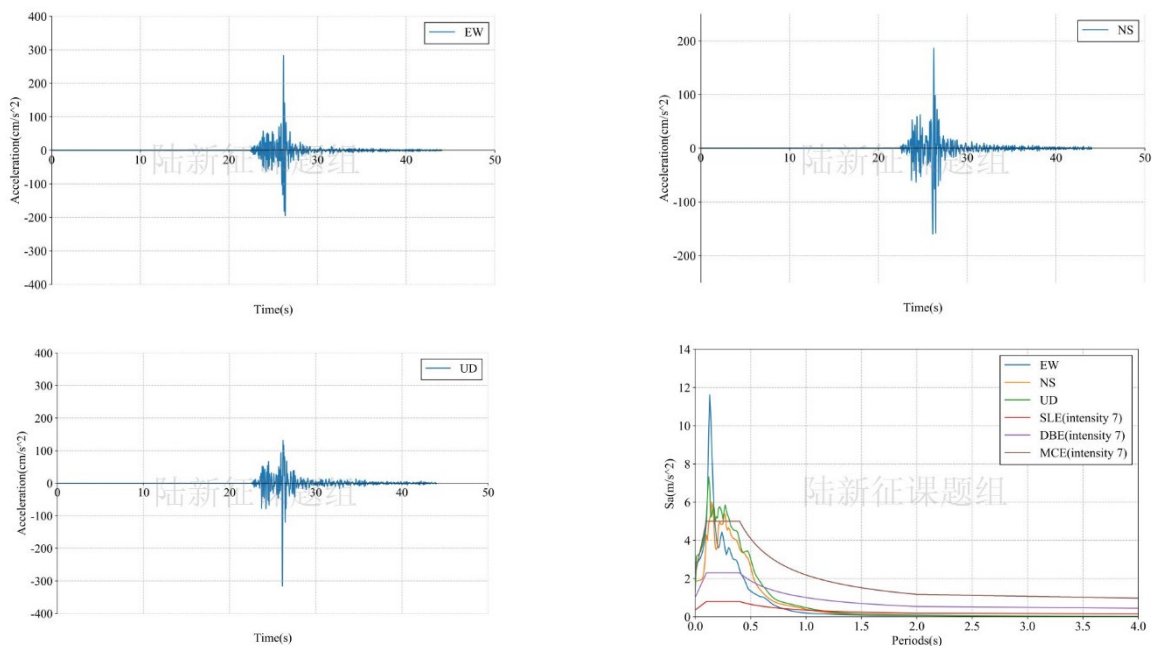


Figure 1 Waveform and response spectra of the recorded ground motions with maximal destructive capacity

3. Damage analysis of the target region subjected to the recorded ground motions

Using the real-time ground motions obtained from the strong motion networks and the **city-scale nonlinear time-history analysis**, the damage ratios of buildings located in different places can be obtained. The building damage distribution and the human feeling distribution near to different stations are shown in Figure 2 and Figure 3, respectively. These outcomes can provide a reference for post-earthquake rescue work

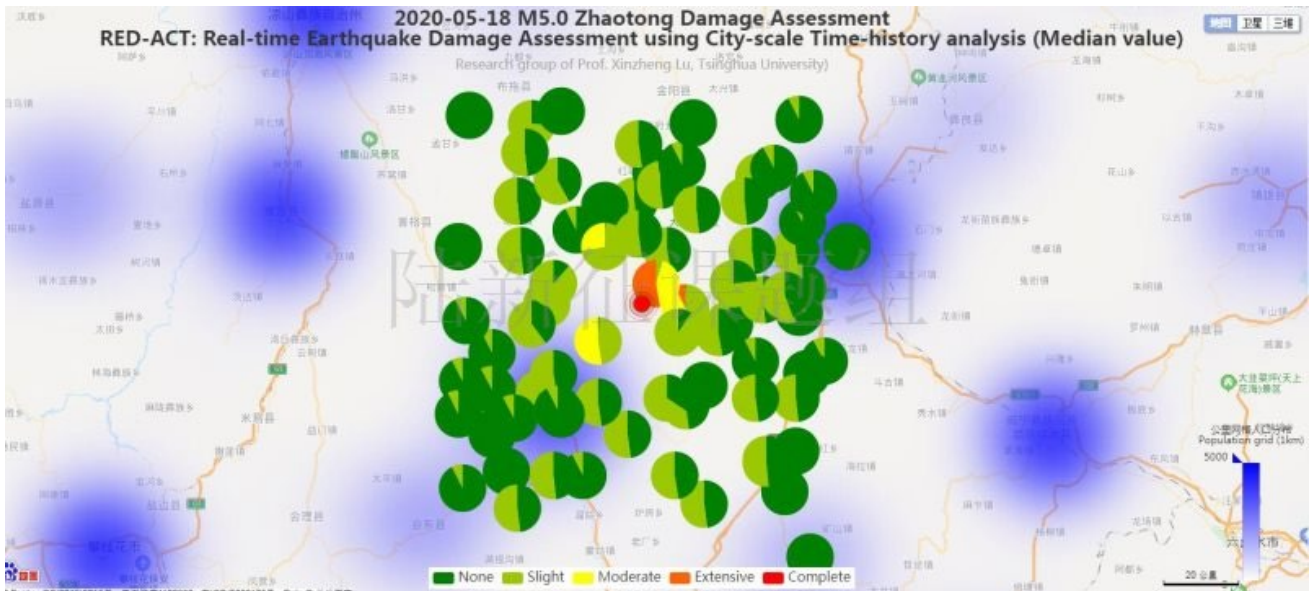


Figure 2 Damage ratio distribution of the buildings near to different stations

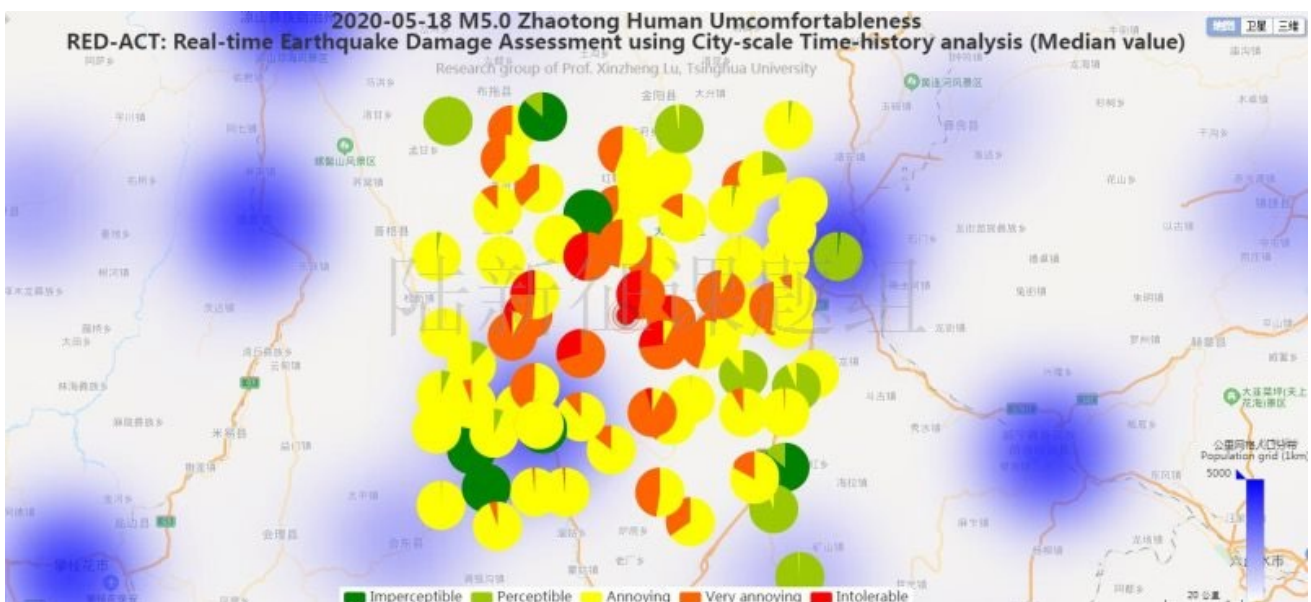
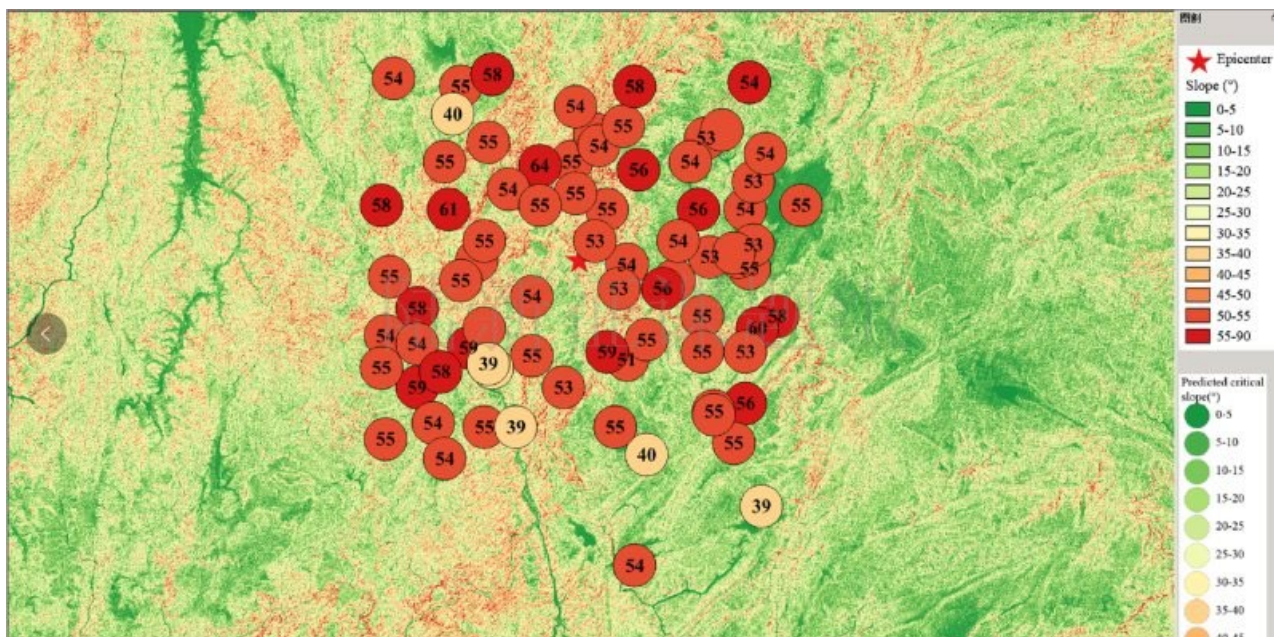


Figure 3 Human feeling distribution near to different stations

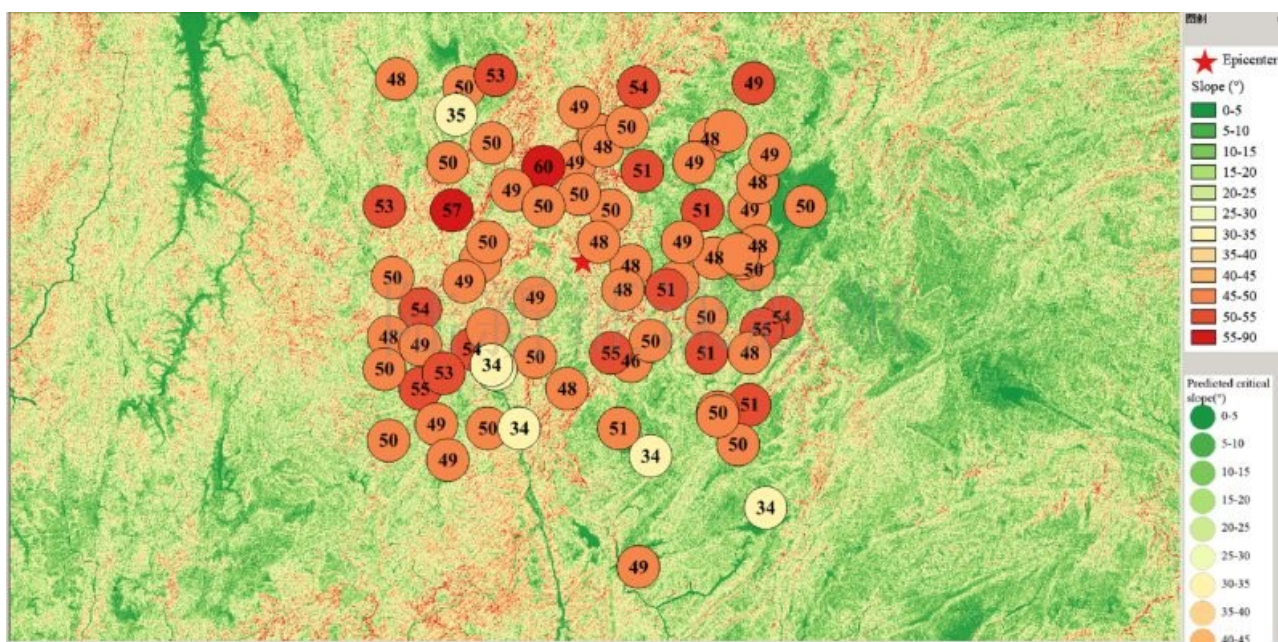
4. Earthquake-induced landslide of the target region subjected to the recorded ground motions

According to local topographic data, lithology data and ground motion records, the distribution of earthquake-induced landslide near to different stations under the different proportions of the landslide slab thickness that is saturated can be calculated, as shown in Figure 4. The basemap shows the distribution of the local slope. The number in the circle

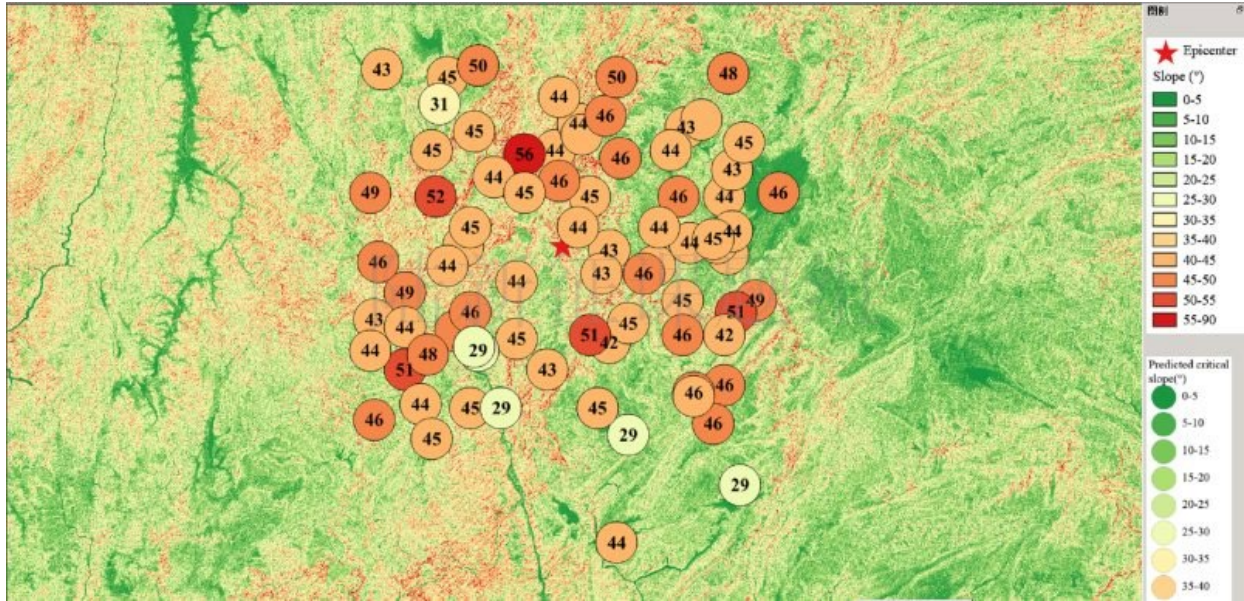
represents the critical slope of the landslide. The earthquake-induced landslide tends to occur with a higher probability when the slope is larger than this threshold value.



(a) The proportion of the landslide slab thickness that is saturated equals 0%



(b) The proportion of the landslide slab thickness that is saturated equals 50%



(c) The proportion of the landslide slab thickness that is saturated equals 90%
 Figure 4 Distribution of earthquake-induced landslide near to different stations

Scientific background of this report can be found at: <http://www.luxinzheng.net/rr.htm>

Table 1 Names and locations of the strong motion stations

No.	Station Name	Longitude	Latitude
1	SMK	102.75	26.86
2	W2603	102.67	26.73
3	W2605	102.79	26.77
4	W2608	102.82	26.68
5	W2610	102.92	26.76
6	W2701	102.90	27.18
7	W2702	102.75	27.06
8	W2704	102.88	26.96
9	W2705	102.68	27.14
10	W2706	102.86	27.13
11	W2707	102.67	26.99
12	W2708	102.66	26.91
13	W2709	102.75	26.97
14	W2711	102.81	26.90
15	W2803	102.69	27.64
16	W2804	102.66	27.32
17	W2901	102.82	27.43
18	W2902	102.86	27.62
19	W2905	102.83	27.31
20	W2907	102.93	27.48
21	W2908	102.94	27.65

22	W2909	102.84	27.55
23	W3002	103.14	27.43
24	W3003	103.06	27.42
25	W3005	103.20	27.50
26	W3007	103.15	27.57
27	W3706	102.94	27.65
28	C0202	103.21	27.47
29	C0203	103.27	27.52
30	C0204	103.31	27.41
31	C0205	103.58	27.31
32	C0206	103.60	27.38
33	C0213	103.63	27.45
34	C0214	103.48	27.49
35	C0216	103.66	27.04
36	C2101	103.44	27.43
37	C2102	103.46	27.31
38	C2103	103.23	27.31
39	C2104	103.28	27.17
40	C2105	103.40	27.13
41	C2106	103.47	27.04
42	C2107	103.61	27.01
43	C2108	103.59	27.16
44	C2110	103.56	27.19
45	C2111	103.49	27.19
46	C2112	103.41	27.23
47	C2201	102.98	27.36
48	C2202	102.92	27.23
49	C2203	102.92	27.01
50	C2204	102.93	26.92
51	C2205	103.00	26.76
52	C2208	103.25	26.76
53	C2209	103.28	26.93
54	C2210	103.33	26.98
55	C2211	102.93	26.92
56	C2212	103.12	26.86
57	C2213	103.04	26.94
58	C2214	103.26	27.11
59	C2215	103.20	27.23
60	C2216	103.15	27.35
61	C2217	103.06	27.32
62	C2218	103.04	27.09
63	C2501	103.30	27.62
64	C2503	103.52	27.51
65	C2504	103.59	27.63

66	D2603	103.58	26.82
67	D2604	103.58	26.95
68	D2605	103.47	26.95
69	D2606	103.50	26.80
70	D2607	103.33	26.69
71	D2608	103.55	26.72
72	QIJ	102.94	26.91
73	53HYC	103.50	26.79
74	53HZH	103.62	26.56
75	53HZX	103.30	26.41
76	53LDC	103.60	27.22
77	53LDX	103.55	27.20
78	53LLT	103.37	27.11
79	53QJT	102.93	26.92
80	53QJX	103.25	26.76
81	53QQC	103.23	26.95
82	53YML	103.59	27.63
83	53ZTT	103.72	27.32